Doxorubicin-induced cardiomyopathy is mitigated by empagliflozin via the modulation of endoplasmic reticulum stress pathways

AKSHI MALIK[1], ASHIM K. BAGCHI[2], DAVINDER S. JASSAL[1,3] and PAWAN K. SINGAL[1*]

[1]Institute of Cardiovascular Sciences, St. Boniface Hospital Albrechtsen Research Centre, Department of Physiology and Pathophysiology, University of Manitoba, Winnipeg R2H 2A6, Canada; [2]Department of Pharmaceutical Sciences, College of Pharmacy, University of Arkansas for Medical Sciences, Little Rock, AR 72205, USA; [3]Section of Cardiology, Department of Internal Medicine, Max Rady College of Medicine, Rady Faculty of Health Sciences, St. Boniface Hospital, Winnipeg, Manitoba R2H 2A6, Canada

Received November 23, 2023; Accepted February 8, 2024

DOI: 10.3892/mmr.2024.13198

Abstract. Doxorubicin (Dox) exhibits a high efficacy in the treatment of numerous types of cancer. However, the beneficial cytotoxic effects of Dox are often accompanied by an increase in the risk of cardiotoxicity. Oxidative stress (OS) plays a key role in Dox-induced cardiomyopathy (DIC). OS in cardiomyocytes disrupts endoplasmic reticulum (ER) function, leading to the accumulation of misfolded/unfolded proteins known as ER stress. ER stress acts as an adaptive mechanism; however, prolonged ER stress together with OS may lead to the initiation of cardiomyocyte apoptosis. The present study aimed to explore the potential of an anti-diabetic drug, empagliflozin (EMPA), in mitigating Dox-induced ER stress and cardiomyocyte apoptosis. In the present study, the effects of 1 h pretreatment of EMPA on Dox-treated cardiomyocytes isolated from Sprague-Dawley rats were investigated. After 24 h, EMPA pre-treatment promoted cell survival in the EMPA + Dox group compared with the Dox group. Results of the present study also demonstrated that EMPA mitigated overall ER stress, as the increased expression of ER stress markers was reduced in the EMPA + Dox group. Additionally, OS, inflammation and expression of ER stress apoptotic proteins were also significantly reduced following EMPA pre-treatment in the EMPA + Dox group. Thus, EMPA may exert beneficial effects on Dox-induced ER stress and may exhibit potential changes that can be utilised to further evaluate the role of EMPA in mitigating DIC.

Correspondence to: Dr Davinder S. Jassal, Section of Cardiology, Department of Internal Medicine, Max Rady College of Medicine, Rady Faculty of Health Sciences, St. Boniface Hospital, 409 Tache Avenue, Winnipeg, Manitoba R2H 2A6, Canada
E-mail: djassal@sbgh.mb.ca

*Deceased

Abbreviations: ATF, activating transcription factor; Dox, doxorubicin; DIC, doxorubicin-induced cardiomyopathy; EMPA, empagliflozin; ER, endoplasmic reticulum; GRP78, glucose-regulated protein 78; IRE, inositol-requiring enzyme; OS, oxidative stress; PDI, protein disulphide-isomerase; PERK, protein kinase-like ER kinase; ROS, reactive oxygen species; SGLT2, sodium-glucose cotransporter-2; STAT, signal transducer and activator of transcription; UPR, unfolded protein response; XBP1, X-box binding protein 1

Key words: DIC, ER stress, inositol-requiring kinase 1α, EMPA

Introduction

Doxorubicin (Dox) is a potent anticancer drug that carries the risk of cardiotoxicity in cancer patients (1,2). The exact underlying mechanisms of Dox-induced cardiomyopathy (DIC) remain elusive, making it difficult to predict or prevent the associated adverse cardiovascular side effects. Numerous molecular mechanisms are known to be involved in DIC, including oxidative stress (OS) (2,3). Dox mediated an increase in reactive oxygen species (ROS) and a decrease in endogenous antioxidants, resulting in OS and the disruption of cell homeostasis, ultimately leading to cell death (4). Among the Dox-induced cellular changes, most remarkable is the dilation of the endoplasmic reticulum (ER) (5,6). Disruption of the ER structure is associated with changes in protein synthesis, folding and translocation, as well as calcium cycling and excitation-contraction coupling in the heart (7,8).

Stress and/or pathological stimuli, such as OS, results in the accumulation of unfolded and/or misfolded proteins in the ER, referred to as ER stress. When ER stress is mild and transient, ER adaptive responses are activated to maintain ER functioning and homeostasis. ER stress activates the unfolded protein response (UPR) through three ER transmembrane sensor proteins: i) Protein kinase-like ER kinase (PERK) (9); ii) activating transcription factor 6α (ATF6α) (10); and iii) inositol-requiring kinase 1α (IRE1) (11). Upon mediation of adaptive responses, luminal ER chaperone, glucose-regulated protein 78 (GRP78) dissociates from PERK, IRE1 and

ATF6α, allowing the activation of their downstream pathways. Subsequent activation leads to the upregulation of ER chaperones and protein foldases, and induces the expression of various genes, including X-box binding protein 1 (XBP1). The unconventional splicing of XBP1 mRNA generates spliced XBP1 (XBP1s) that subsequently plays an essential role in further upregulation of chaperones, such as glucose-regulated protein 94 (GRP94), GRP78 and/or protein disulfide-isomerase (PDI) (8,12). However, when ER stress is severe, UPR fails to restore ER homeostasis. ER stress initiates apoptotic signaling pathways via CCAAT/enhancer homologous protein (CHOP), caspase-12 activation, phosphorylation of c-JUN NH2-terminal kinase (JNK) and pro-apoptotic gene expression, which play an essential role in the progression of DIC and cardiomyocytes loss (13,14).

Empagliflozin (EMPA) is a sodium-glucose co-transporter 2 (SGLT-2) inhibitor that is used to decrease blood glucose levels and sodium load in diabetic patients (15). Results of the EMPA-REG OUTCOME trial demonstrated that EMPA reduced the risk of hospitalization for heart failure and cardiovascular death in the EMPA-REG OUTCOME trial (16). Additional clinical trials, including the EMPEROR-Reduced and EMPEROR-Preserved trials, reported cardio-renal benefits of EMPA in the non-diabetic population (17-19). As per the Canadian Cardiovascular Society heart failure guidelines, SGLT-2 inhibitors have now been included as first-line therapy in the setting of heart failure with reduced ejection fraction (20). In addition, results of pre-clinical studies demonstrated the utility of EMPA and other SGLT-2 inhibitors in the prevention of DIC (21,22). Dapagliflozin was reported to attenuate DIC in a murine diabetic model (22) via inhibition of ER stress. Moreover, Sabatino *et al* (21) suggested that the beneficial effects of EMPA on DIC may be independent of its glycemic control.

Results of a previous study by the authors and other studies demonstrated that the mitigation of ER stress reduces the detrimental effects of Dox and cardiomyocyte loss (23-26). However, the effects of EMPA in mitigating Dox-induced ER stress as well as the molecular pathways involved are unknown. The present study aimed to examine the potential role of EMPA in mitigating Dox-mediated ER stress injury in the *in vitro* setting using isolated cardiomyocytes. It was demonstrated that EMPA reduces overall ER-stress in Dox treated cardiomyocytes. Additionally, the present novel results confirmed that these changes were due to increased expression of an ER transmembrane protein, inositol-requiring kinase 1α (IRE1), which plays an essential role in maintaining ER homeostasis and inhibiting inflammation and ER-initiated apoptosis upon Dox insult.

Materials and methods

Cardiomyocyte isolation and treatment. The guidelines of the Canadian Council on Animal Care were followed for all animal procedures, and the present study was approved [(approval no. 22-012 (AC11739)] by the Animal Protocol Review Committee at the University of Manitoba (Winnipeg, Canada). Male Sprague Dawley rats (n=10; ~8 weeks-old; weight, 200±10 g) were ordered from Charles River laboratories and shipped to our facility in a climate-controlled vehicle. Rats were housed in a temperature-regulated room (22-24˚C) on a 12/12-h light-dark cycle, and had *ad libitum* access to standard chow and water. After 1 week of conditioning, rats were administered the following anesthetic agents intraperitoneally (ketamine 90 mg/kg and xylazine 10 mg/kg) prior to euthanasia. Subsequently, the hearts were removed for cardiomyocyte isolation using the standard Langendorff apparatus, as previously described (23,24). In total, ~10^6 cells were plated in 10-cm laminin-coated polystyrene tissue culture plates (cat. no. CLS430167; Corning, Inc.) with 10% fetal bovine serum (FBS; Thermo Fisher Scientific, Inc.) and streptomycin/penicillin (100 U/ml) in M199 culture media (Sigma-Aldrich; Merck KGaA) at 37˚C in 5% CO_2 with 95% O_2. After 2 h primary incubation, dead cells were removed by washing with M199 culture media and viable cells were incubated overnight with 0.5% FBS under the same incubation conditions. The following morning, culture plates were randomly divided into four treatment groups as follows: Control (cardiomyocytes cultured in M199 +0.5% FBS); EMPA (500 nM; cat. no. 22369-1; Cayman Chemical Company); Dox (10 μM; Pfizer, Inc.); and Dox + EMPA, for 24 h. For the combination group of Dox + EMPA, cells were treated with EMPA for 1 h prior to the addition of Dox.

Cell viability. Isolated cardiomyocytes were incubated for different times (0, 6, 12 and 24 h) to determine time- and treatment-dependent viability. An MTT [3-(4,5-dimethylthiazol-2-yl)-2,5-diphenyltetrazolium bromide] assay was performed after each treatment period. Briefly, cardiomyocytes (~10^4 cells/well) were plated on 96-well plates for a specific time, and 5 mg/ml MTT was subsequently added to each well for 2 h at 37˚C. After 2 h incubation, formazan crystals were observed. Once the crystallization was >90%, MTT was removed, and 150 μl of dimethyl sulfoxide was added to each well and mixed in the dark. The absorbance of each well was subsequently recorded at 570 nm using a Cytation 5 Cell Imaging Multi-Mode Reader (RRID:SCR_019732; BioTek Instruments, Inc.).

Protein estimation and western blot analysis. At the end of the treatment period, cardiomyocytes were washed with PBS and centrifuged at 12,000 x g for 10 min at room temperature (RT). The cell pellet was resuspended in ice cold RIPA buffer (cat. no. 89900; Thermo Fisher Scientific, Inc.) with Pierce protease and phosphatase inhibitors, (cat. no. A32959; Pierce; Thermo-Fisher Scientific, Inc.), 1 mM phenylmethylsulfonyl fluoride, and DTT overnight at -20˚C. After overnight incubation, samples were sonicated using a water bath sonicator. Sonicated samples were subsequently centrifuged at 12,000 x g for 15 min at 4˚C. The supernatant was used to determine total protein concentration as per the Bradford dye-binding method using BSA as a standard (Bio-Rad Laboratories, Inc.) using a microwell plate reader (Cytation 5; BioTek Instruments, Inc.). Total protein was stored at -20˚C until further analysis.

A total of 20-40 μg of protein was separated using electrophoresis on 8-12% SDS-polyacrylamide gels at 80 mV. The separated proteins were subsequently transferred onto a PVDF membrane for 90 min at constant 200 mA in a cold

room. Membranes were subsequently blocked in 5% BSA and washed with Tris-buffered saline plus 0.1% Tween-20 (TBST) blocking buffer for 1 h at RT. After blocking, membranes were incubated with the respective antibodies for either 1.5 h at RT or overnight at 4˚C on a rocker. Membranes were subsequently washed with TBST (3 washes 10 min each) and incubated with horseradish peroxidase (HRP)-conjugated anti-rabbit IgG (1:5,000; cat. no. W401B; RRID: AB_430833; Promega Corporation) or HRP-conjugated anti-mouse IgG secondary antibodies (1:5,000; cat. no. 170-6516; RRID: AB_11125547; Bio-Rad Laboratories, Inc.) for 1 h at RT. Protein bands were visualized using the Pierce ECL Plus Western Blotting Substrate (PerkinElmer, Inc.) at different exposure times on a Chem Doc imager (BioRad Laboratories, Inc.). Densitometric analysis was performed using Image Lab 6.0 (Bio-Rad Laboratories, Inc.) and GAPDH was used for normalization for each sample.

Primary antibodies were as follows: Anti-Caspase-12 (1:2,000; cat. no. ab62484; RRID: AB_955729; Abcam); anti-K-Lysine, D-Aspartic acid, E-Glutamic acid and L-Leucine sequence (1:1,000; cat. no. ab176333; RRID: AB_2819147; Abcam) which is used to target GRP94, GRP78 and PDI; anti-XBP1 (1:500; cat. no. ab37152; RRID: AB_778939; Abcam); anti-ATF6 (1:5,000; cat. no. 24169-1-AP; RRID: AB_2876891; ProteinTech Group, Inc.); anti-PERK (1:500; cat. no. 20582-1-AP; RRID: AB_10695760; ProteinTech Group, Inc.); anti-IRE1 (1:1,500; cat. no. 20582-1-AP; RRID: AB_1069#5760; ProteinTech Group, Inc.); anti-JNK1 + JNK2 + JNK3 (1:1,000; cat. no. ab179461; RRID: AB_2744672; Abcam); anti-phosphorylated (p-)JNK1 + JNK2 + JNK3 [T183 + T183 + T221 (1:500; cat. no. ab124956; RRID: AB_10973183; Abcam); anti-sodium-glucose cotransporter-2 (SGLT2; 1:1,000; cat. no. ab37296; RRID: AB_777895; Abcam) and anti-GAPDH (1:4,000; cat. no. 2118; RRID: AB_561053; Cell Signaling Technology, Inc.).

Reverse transcription-quantitative (RT-q) PCR. Aurum™ Total RNA Mini kit (cat. no. 7326820; BioRad Laboratories, Inc.) was used to isolate total RNA in the cell culture hood according to the manufacturer's protocols. Extracted RNA was quantified using nanodrop (Nanodrop Lite; Thermo Fisher Scientific, Inc.). Total RNA was reverse transcribed into cDNA (40 ng) using High-Capacity cDNA Reverse Transcription kit with RNase Inhibitor as per manufacturer's instructions (cat. no. 4374966; Thermo Fisher Scientific, Inc.) on the T100 Thermal Cycler (RRID:SCR_021921; BioRad Laboratories, Inc.). RT-qPCR reactions were prepared using 22.5 ng/μl of cDNA template and 500 nM of forward and reverse primers to a final volume of 10 μl. RT-PCR amplification was performed using a QuantStudio 3 Real Time PCR System (RRID:SCR_020238; Thermo Fisher Scientific, Inc.) with Luna Universal Master Mix (cat. no. M3003; New England Biolabs, Inc.). The program was set up to have initial denaturation at 95˚C for 60 sec, followed by 40 cycles of denaturation at 95˚C for 15 sec, and extension at 60˚C for 30 sec. A continuous melt curve was subsequently produced from 60-95˚C for ~20 sec. mRNA levels were quantified using the $2^{-\Delta\Delta Cq}$ method and normalized to the internal reference gene GAPDH (27). Primer sequences are displayed in Table I.

Table I. Rat-specific primer sequences used for reverse transcription-quantitative PCR.

Gene name	Primer sequence (5'→3')
XBP1	F: ACGAGAGAAAACTCATGG
	R: ACAGGGTCCAACTTGTCC
IL-10	F: AGTGGAGCAGGTGAAGAATGA
	R: CAGTAGATGCCGGGTGGTT
TNFα	F: ATGGGCTCCCTCTCATCAGT
	R: GCTTGGTGGTTTGCTACGAC
TGFβ	F: GCGGACTACTACGCCAAAGA
	R: TGCTTCCCGAATGTCTGACG
STAT-3	F: TCGGAAAGTATTGTCGCCCC
	R: GACATCGGCAGGTCAATGGT
GAPDH	F: CATCAACGACCCCTTCATTGACCTCA ACTA
	R: TCCACGATGCCAAAGTTGTCATGG

F, forward; R, reverse.

Glucose uptake assay. Glucose Uptake Assay kit (cat. no. ab136956; Abcam) was used to record glucose uptake, according to the manufacturer's instructions. Briefly, ~10^4 cells were plated in a 96-well flat bottom plate and treated as previously described. At the end of the treatment period, cells were washed three times with PBS and Tyrode's solution with 10 mmol/l mannitol was added for 45 min to starve cells of glucose. Subsequently, 2-deoxyglucose (2-DG), which is structurally similar to glucose, was added to all cells excluding the respective negative controls, and incubated for 30 min. Cells were subsequently washed with PBS to remove exogenous 2-DG and lysed using extraction buffer at -80˚C. After repeating freeze/thaw cycles, cell lysates were boiled at 80˚C for 45 min. Cell lysate was cooled on ice for 5 min and then neutralised using neutralization buffer. Following centrifugation, the supernatant was collected and mixed with reaction mix and 2-DG uptake assay buffer and incubated in the dark for 40 min. Fluorescence of accumulated 2-DG-6-phosphate (2-DG6P) was recorded with excitation/emission at 535/587 nm using the Cytation 5 Cell Imaging Multi-Mode Reader (RRID:SCR_019732; BioTek Instruments, Inc.). Final 2-DG uptake was calculated using a 2-DG6P standard curve.

2',7'-dichlorodihydrofluorescein diacetate (H_2DCFDA) assay. H_2DCFDA dye (cat. no. D399; Invitrogen; Thermo Fisher Scientific, Inc.) was used to measure overall OS in different treatment groups. Briefly, ~10^4 cells were plated in 96-well flat bottom plates and treated as previously described. At the end of the treatment period, cells were washed three times with PBS +0.1% FBS and 5 μM dye was added in each well. Plates were incubated in the dark for 45 min to allow diffusion of dye into the cell. After three washes with PBS +0.1% FBS, fluorescence was recorded with excitation/emission at 485/535 nm using the Cytation 5 Cell Imaging Multi-Mode Reader (RRID:SCR_019732; BioTek Instruments, Inc.). Images were captured at a magnification of x20.

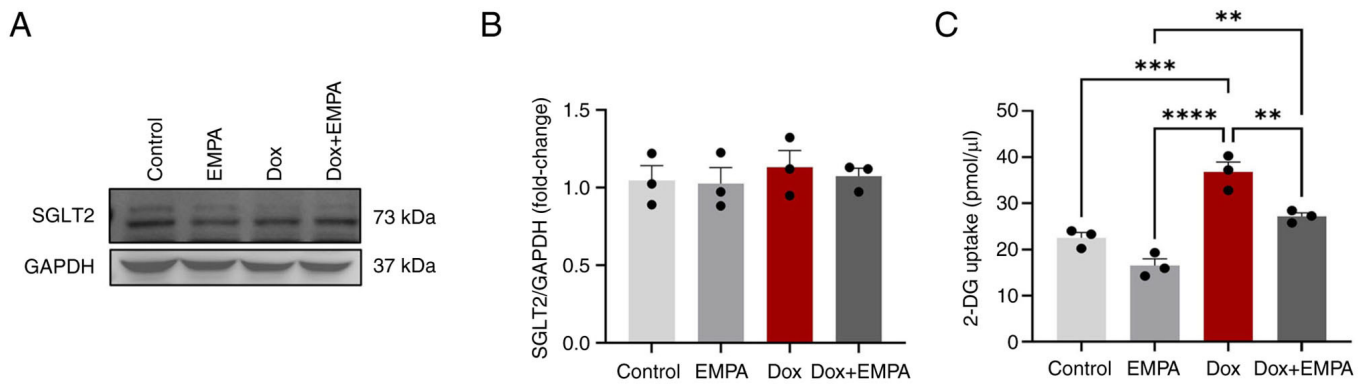

Figure 1. Expression of SGLT2 and the effects of EMPA on 2-DG uptake. Cardiomyocytes were treated with either Dox (10 μM), EMPA (500 nM) or Dox + EMPA for 24 h. (A) SGLT2 protein using SGLT2 antibody (1:500). GAPDH is shown as a loading control. (B) Densitometric analysis of SGLT2/GAPDH fold change. (C) Quantification of cellular 2-DG absorption in treated cardiomyocytes. Data are presented as the mean ± SEM, using three individual biological samples repeated in duplicate. **P<0.005, ***P<0.0005 and ****P<0.00005. EMPA, empagliflozin; 2-DG, 2-deoxyglucose; Dox, Doxorubicin; SGLT2, sodium-glucose co-transporter 2.

Statistical analysis. All experiments were performed in duplicate for each treatment group for a total of 3-5 individual biological samples. Data are expressed as the mean ± SEM. Comparisons between treatment groups were carried out using one-way ANOVA, and Tukey-Kramer's test was performed to identify differences between groups. Data analysis was performed using GraphPad Prism (version 8.0; GraphPad Software, Inc.; Dotmatics). P<0.05 was considered to indicate a statistically significant difference.

Results

Expression of SGLT2 and effects of EMPA on 2-DG uptake. As EMPA inhibits SGLT2 transporters, isolated cardiomyocytes were treated with 10 μM Dox for 24 h with or without EMPA, and SGLT2 protein expression was investigated using western blot analysis (Fig. 1A). Although the baseline expression of SGLT2 was detected (both the 73 kDa SGLT-2 and its cleavage fragments) (Fig. 1A), the relative expression of SGLT2 among different treatment groups was not different from each other (Fig. 1B). As SGLT2 was expressed in adult rat cardiomyocytes, the primary function of EMPA was evaluated. Subsequently, a 2-DG uptake assay was performed because of its structural similarity to glucose. 2-DG is taken up by glucose transporters and metabolized to 2-DG-6-phosphate (2-DG6P). However, it cannot be further metabolized, and therefore accumulates within cells. Using the relative fluorescence of oxidized 2-DG6P, 2-DG6P uptake was determined amongst treatment groups. Results of the present study demonstrated that EMPA-treated cardiomyocytes exhibited significantly low levels of 2-DG6P uptake, compared with Dox, and Dox + EMPA groups (Fig. 1C). Notably, the Dox group exhibited a higher 2-DG uptake, compared with the control group (Fig. 1C). However, no significant changes were observed between the Dox + EMPA and control groups (Fig. 1C).

Dox-induced expression of ER stress markers and their mitigation by EMPA. ER stress leads to the overexpression of UPR chaperones which were significantly higher following Dox treatment. Dox treatment for 24 h increased the protein expression of GRP94, GRP78 and PDI compared with the control and EMPA groups (Fig. 2A-D). In Dox + EMPA-treated cardiomyocytes, increases in protein expression were significantly inhibited following EMPA treatment, compared with the Dox group (Fig. 2A). Notably, GRP94, RP78 and PDI expression levels were reduced following treatment with EMPA; however, these changes were not significant.

EMPA-induced changes in UPR signaling proteins. Upon induction of ER stress, UPR signaling proteins (PERK, IRE1 and ATF6α) are activated. Results of the present study demonstrated that Dox treatment significantly reduced the expression of PERK and IRE1, compared with the control group (Fig. 3A-D). Notably, pre-treatment with EMPA prevented the downregulation of IRE1 by Dox, and the observed expression levels were not significant compared with the control group (Fig. 3C and D). However, EMPA exerted no significant effect on PERK expression (Fig. 3A and B) in the Dox + EMPA group. Dox activates ATF6α cleavage, and results of the present study revealed an increase in the activated cleaved ATF6α fragment (Fig. 3E and F). Increased expression of active ATF6α was prevented following treatment with EMPA.

EMPA-induced changes in XBP1 mRNA and protein expression levels. XBP1 plays an essential role in mediating UPR function and is a transcription factor for genes required by UPR. Dox treatment significantly increased *XBP1* mRNA expression levels, compared with the control and EMPA groups (Fig. 4C). However, pre-treatment with EMPA exerted no effect on *XBP1* mRNA, and the expression levels remained high. Results of the present study also demonstrated that Dox treatment caused a 1.5-fold increase in XBP1s/XBP1u protein expression, and these levels were significantly reduced following treatment with EMPA (Fig. 4A and B). However, XBP1u protein expression levels remained unchanged in all groups, excluding the Dox group. Results of the present study demonstrated that the expression of XBP1s/XBP1u was high in Dox-treated cardiomyocytes, and expression returned to levels similar to that of the control following treatment with EMPA (Fig. 4A and B).

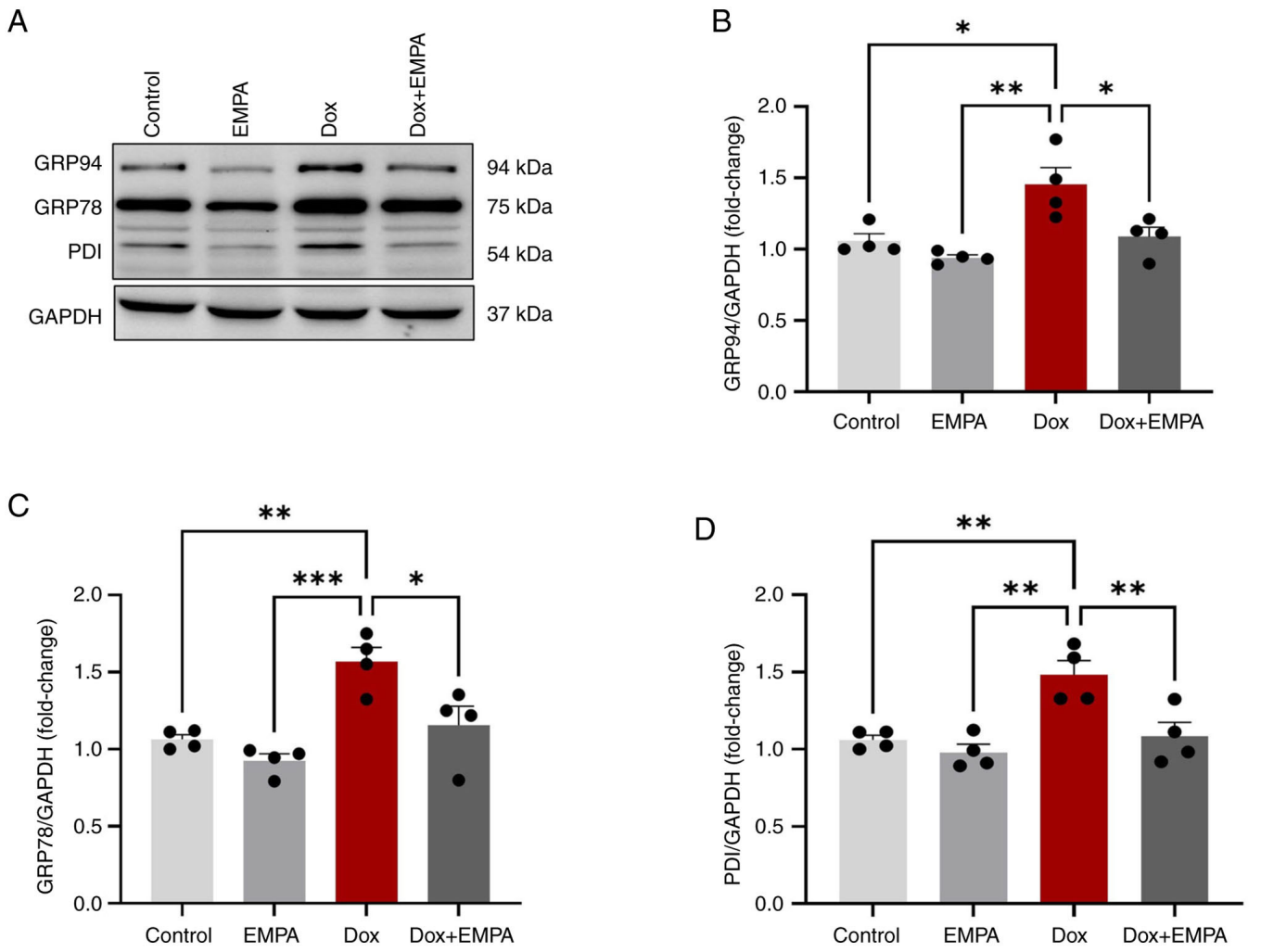

Figure 2. Protein expression of unfolded protein response chaperones. Cardiomyocytes were treated with either Dox (10 μM), EMPA (500 nM) or Dox + EMPA for 24 h. (A) K-Lysine, D-Aspartic acid, E-Glutamic acid and L-Leucine sequence antibody was used to determine GRP94, GRP78 and PDI expression levels. (B-D) Densitometric analysis of respective proteins using GAPDH as the loading control. Data are presented as the mean ± SEM, using four individual biological samples repeated in duplicate. *P<0.05, **P<0.005 and ***P<0.0005. Dox, Doxorubicin; EMPA, empagliflozin; PDI, protein disulfide-isomerase; GRP, glucose-regulated protein.

Effects of EMPA on ER stress-induced apoptosis. When cells fail to recover from ER stress, ER initiates apoptosis through the JNK-pathway, leading to the activation of caspases. Results of the present study demonstrated that ER resident caspase-12 was activated and the levels of cleaved/total caspase-12 were significantly higher following Dox treatment. However, pre-treatment with EMPA reduced the activation of caspase-12 through preventing cleavage (Fig. 5A and B). Results of the present study also demonstrated a significant increase in the phosphorylation of JNK (p-JNK) following treatment with Dox, compared with the control and EMPA groups (Fig. 5C and D). However, the expression of p-JNK was significantly reduced in the in Dox + EMPA group, compared with the Dox group.

Moreover, the viability of cardiomyocytes was measured at 3, 12, 24 and 48 h using an MTT assay (Fig. 5E). Results of the present study demonstrated that Dox significantly reduced cell viability to 55% at 24 h, and ~40% of cardiomyocytes survived for 48 h. Pre-treatment with EMPA rescued cardiomyocytes from Dox-induced cell death, and >80% of cardiomyocytes were viable at 24 h. After 48 h, EMPA-treated cardiomyocytes exhibited ~75% viability, and this was significantly higher than the control group (Fig. 5E).

EMPA protects against Dox-induced OS and inflammation. Dox-induced production of ROS and excessive OS lead to cardiomyopathy. Thus, ROS production was recorded following Dox treatment with or without EMPA. Results of the present study demonstrated a >4-fold increase in ROS production following 24 h Dox treatment (Fig. 6A and B), and pre-treatment with EMPA significantly reduced OS.

Dox-induced inflammation plays an essential role in cardiac remodelling and the development of heart failure. Dox treatment for 24 h significantly increased mRNA expression levels of the pro-inflammatory cytokine, *TNFα,* and pro-fibrosis cytokine, *TGFβ,* and reduced the expression levels of inflammation-induced cardioprotective signal transducer and activator of transcription-3 (*STAT-3*) and anti-inflammatory cytokine, *IL-10*. In Dox-treated cardiomyocytes, pre-treatment with EMPA significantly reduced the expression of both *TNFα* and *TGFβ*, compared with the

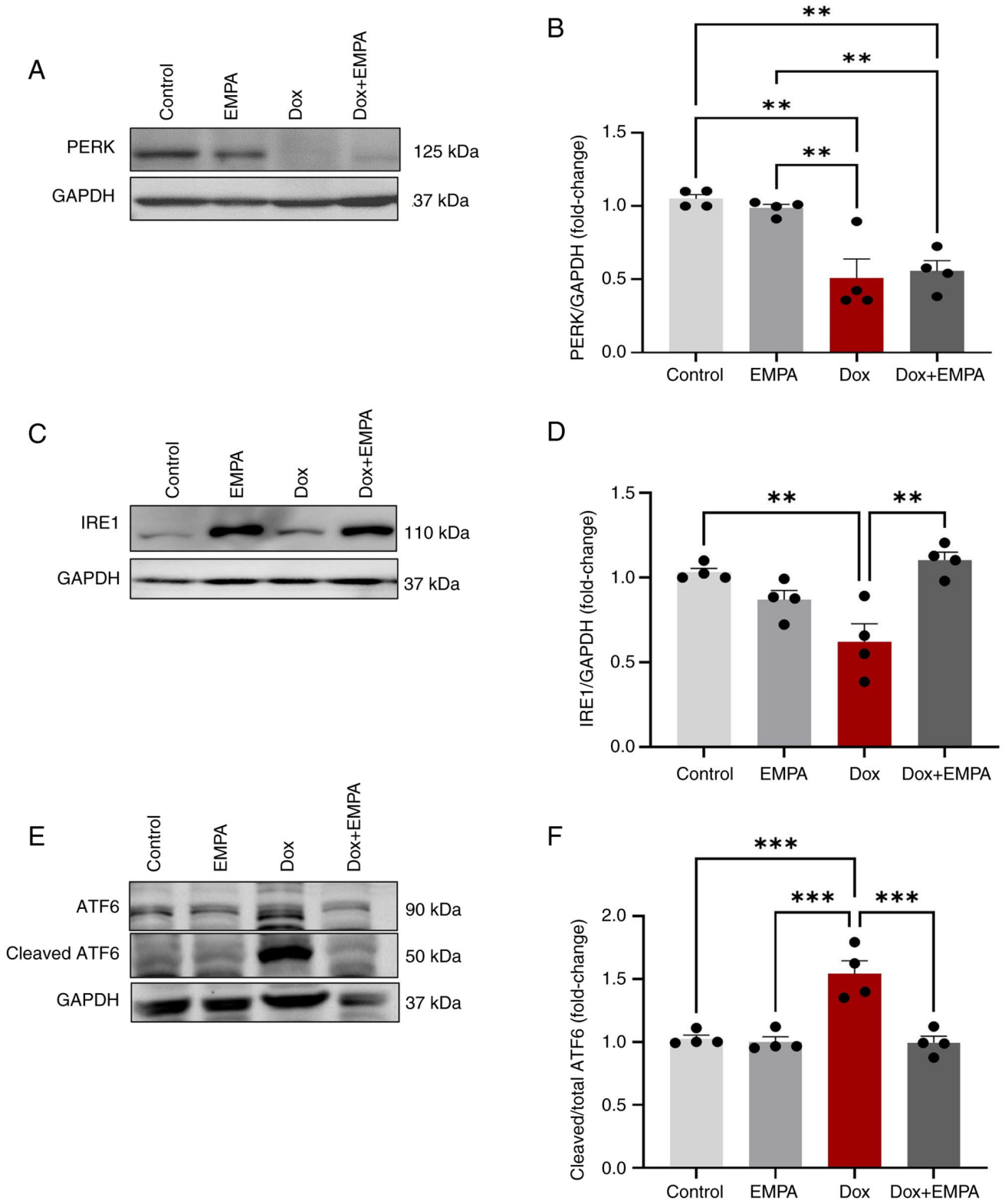

Figure 3. Expression of unfolded protein response signaling proteins. Cardiomyocytes were treated with either Dox (10 μM), EMPA (500 nM) or Dox + EMPA for 24 h. (A) PERK protein expression. (B) Densitometric analysis of PERK using GAPDH as the loading control. (C) IRE1 protein expression. (D) Densitometric analysis of IRE1 using GAPDH as the loading control. (E) ATF6 and cleaved ATF6 protein expression. (F) Densitometric analysis of cleaved/total ATF6. Data are presented as the mean ± SEM, using four individual biological samples repeated in duplicate. **P<0.005 and ***P<0.0005. Dox, Doxorubicin; EMPA, empagliflozin; PERK, protein kinase-like endoplasmic reticulum kinase; IRE1, inositol requiring kinase 1α; ATF6α, activating transcription factor 6α.

Dox group (Fig. 7A and B). Moreover, Dox promoted inflammation through the significant downregulation of *IL-10* and *STAT-3*; however, treatment with EMPA exerted no effects on the levels of *IL-10*. Notably, the levels of *STAT-3* returned to baseline following treatment with EMPA, compared with the Dox group (Fig. 7C and D).

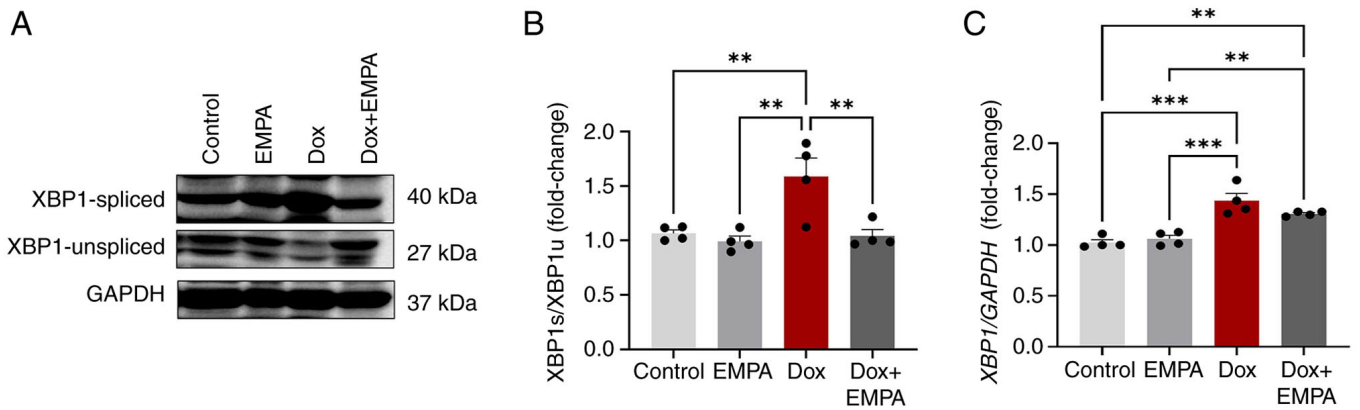

Figure 4. Protein and mRNA expression of XBP1. Cardiomyocytes were treated with either Dox (10 μM), EMPA (500 nM) or Dox + EMPA for 24 h. (A) XBP1 protein expression. (B) Ratio of spliced XBP1(s) and un-spliced XBP1(u) proteins. (C) Relative expression levels of XBP1 mRNA using GAPDH as an endogenous control. Data are presented as the mean ± SEM, using four individual biological samples repeated in duplicate. **P<0.005 and ***P<0.0005. XBP1, X-box binding protein 1; Dox, Doxorubicin; EMPA, empagliflozin.

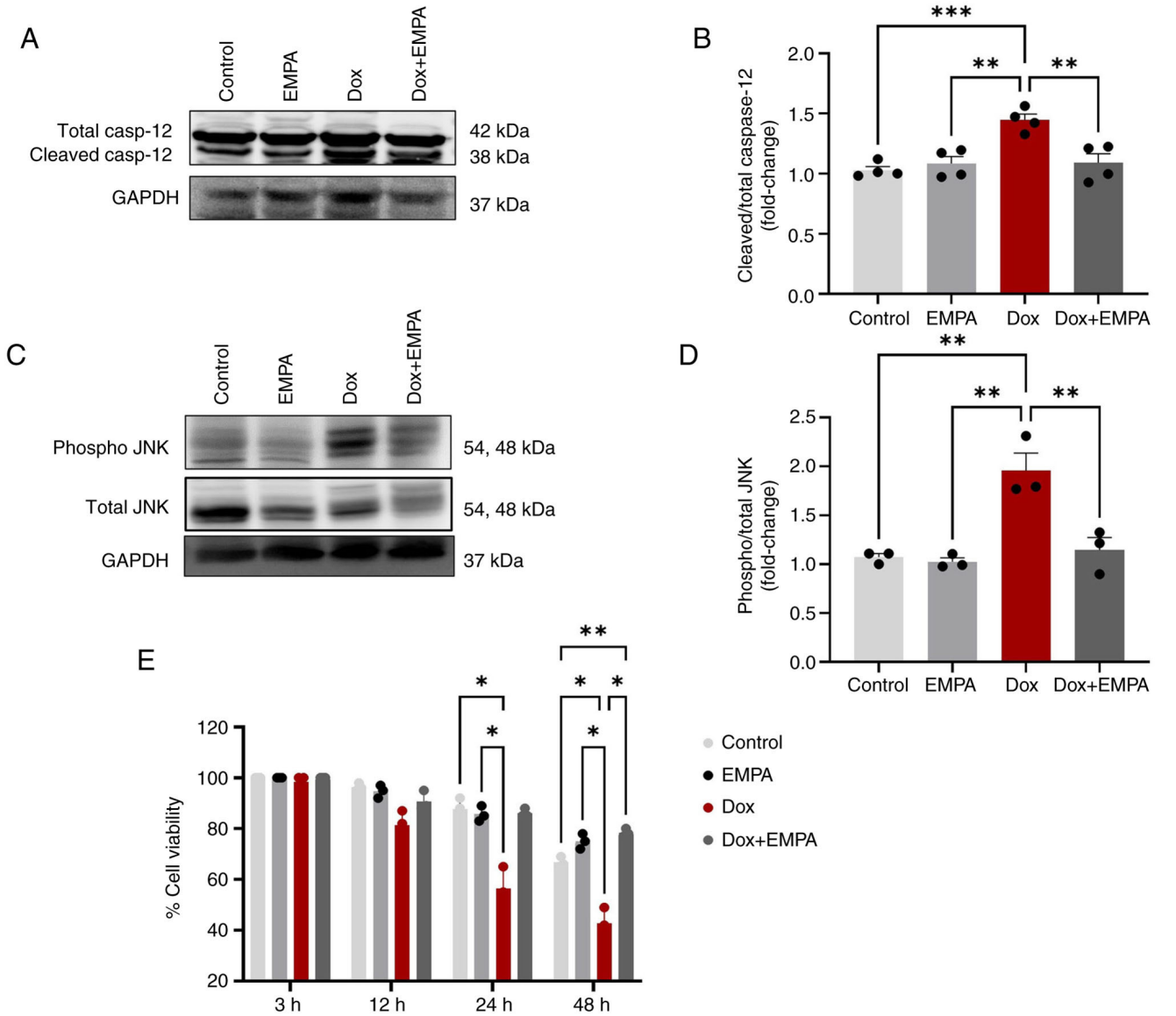

Figure 5. ER stress-induced apoptosis and cell death. Cardiomyocytes were treated with either Dox (10 μM), EMPA (500 nM) or Dox + EMPA for 24 h. (A) Caspase-12 protein expression. (B) Densitometric analysis of cleaved/total caspase-12. (C) Expression levels of p-/total JNK. (D) Densitometric analysis of p-/total JNK protein. (E) Cardiomyocyte viability in different treatment groups at different time points (3-48 h) using an MTT assay. Data are presented as the mean ± SEM, using four individual biological samples repeated in duplicate. *P<0.05, **P<0.005 and ***P<0.0005. ER, endoplasmic reticulum; EMPA, empagliflozin; Dox, Doxorubicin; p-, phosphorylated.

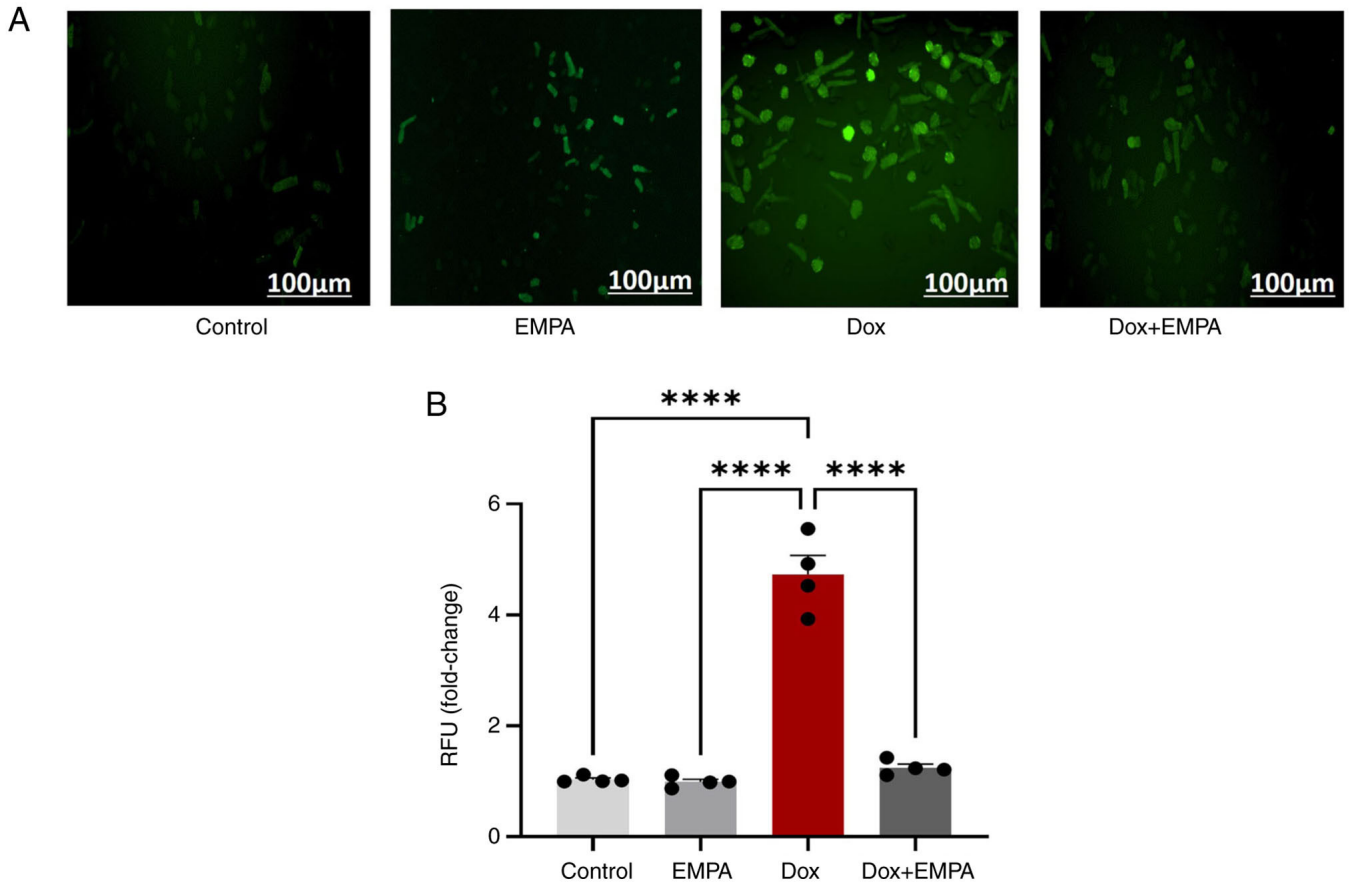

Figure 6. EMPA protects against Dox-induced oxidative stress. Cardiomyocytes were treated with either Dox (10 μM), EMPA (500 nM) or Dox + EMPA for 24 h. (A) ROS production measured using H2DCFDA dye in different treatment groups (magnification, x20; scale bar, 100 μm). (B) Quantification of relative fluorescence unit fold change in different treatment groups. Data are presented as the mean ± SEM, using four individual biological samples repeated in duplicate. ****P<0.00005. EMPA, empagliflozin; Dox, Doxorubicin.

Discussion

EMPA, an SGLT2 inhibitor, was first approved in 2014 for the treatment of diabetes. In 2022, the US Food and Drug Administration expanded the use of EMPA for guideline-directed medical therapy in individuals with heart failure and reduced ejection fraction, irrespective of diabetes status (28). However, the use of EMPA in DIC and identification of its potential cardioprotective mechanism(s) is yet to be explored. The present study aimed to investigate the effects of EMPA pre-treatment on Dox-treated adult primary cardiomyocytes, with a focus on ER stress.

Numerous previous studies have demonstrated the absence of SGLT2 expression in the heart (29,30); however, the results of some studies have reported low expression of SGLT2 in the heart, when compared with expression in the kidney and liver (21,30-34). In the present study, the protein expression of SGLT2 was measured, and expression remained unchanged following Dox treatment in primary cardiomyocytes. To verify the impact of EMPA on the inhibition of glucose absorption, a glucose uptake assay was performed. In 24 h, EMPA had reduced glucose absorption, compared with the Dox group. However, it was not completely inhibited as cardiomyocytes possess other glucose transporters (31,32). Notably, Dox-treated cardiomyocytes exhibited a higher glucose uptake than the control group, confirming the metabolic derangements induced by Dox. Dox impairs oxidative phosphorylation in the heart, and the persistent activation of glycolysis enables cardiomyocytes to meet the energy demand of a failing myocardium (35,36). The ability of EMPA to reduce glucose uptake following Dox treatment may prevent the heart from metabolic imbalances and the associated complications.

The intermediary role of ER stress in Dox-induced apoptosis and myocardial dysfunction have previously been identified (13,24,37). The present study examined the activity of UPR transmembrane proteins and the EMPA-mediated management of ER stress. Dox treatment significantly increased the expression of ER stress markers (GRP94, GRP78 and PDI), and expression of these stress markers was reduced following treatment with EMPA. Notably, PERK and IRE1 protein expression levels are reduced following Dox treatment (13,24). Moreover, EMPA treatment restored IRE1 expression levels. However, EMPA exerted no significant effect on PERK expression. Results of a previous study demonstrated that EMPA inhibited autophagy in myocardial I/R injury through inhibition of the PERK pathway (38). Thus, EMPA-induced low expression of PERK in the Dox + EMPA group, may aid in mitigating Dox-induced autophagy. Results of the present study also demonstrated the high expression of IRE1 (Fig. 3D). The downstream pathway molecule of IRE1, *XBP1,* was explored to further elucidate its involvement in the attenuation of overall ER-stress. IRE1 plays an essential role

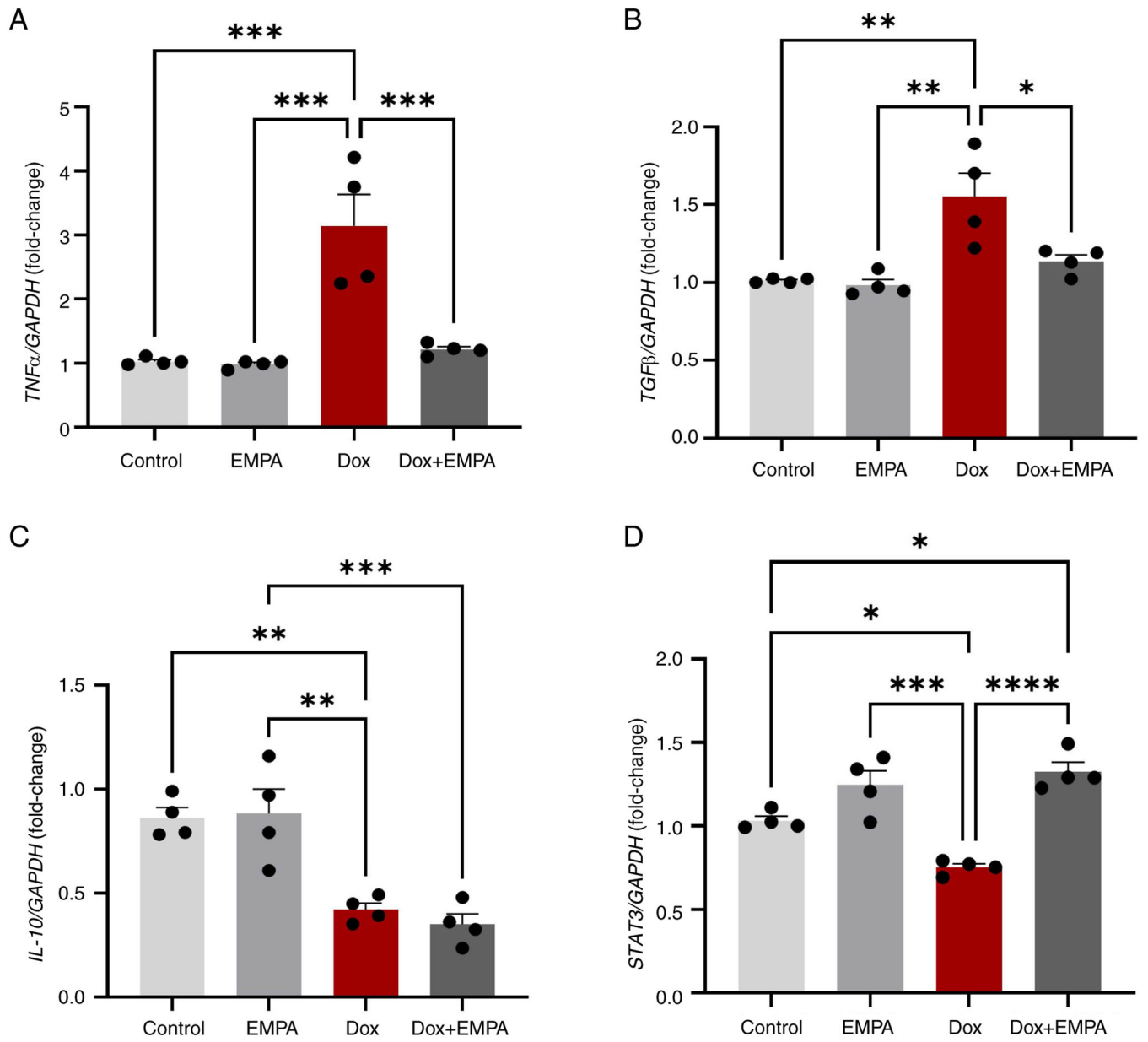

Figure 7. Effects of EMPA on inflammatory markers. Cardiomyocytes were treated with either Dox (10 μM), EMPA (500 nM) or Dox + EMPA for 24 h. (A-D) Relative mRNA expression of inflammatory markers using *GAPDH* as an endogenous control. Data are presented as the mean ± SEM, using four individual biological samples repeated in duplicate. *P<0.05, **P<0.005, ***P<0.0005 and ****P<0.00005. EMPA, empagliflozin; Dox, Doxorubicin.

in inducing the splicing of *XBP1*. Splicing of *XBP1* generates a highly active *XBP1s*, and its negative regulator *XBP1u*. IRE1-XBP1 is the most essential arm of the unfolded protein response that is required for efficient protein folding, maturation and degradation of the misfolded proteins (11,39,40).

When translocated to the nucleus, *XBP1s* aids in the transcription of UPR-associated genes, inflammatory responses, differentiation, and the structural and functional expansion of ER (40,41). Results of previous studies suggested that an increase in *XBP1* levels and the associated splicing may also occur via the ATF6α pathway (10,11,24). Results of the present study demonstrated activation of the ATF6α pathway through cleaved ATF6α expression, and high expression of *XBP1* levels in Dox-treated cardiomyocyte without IRE1 overexpression is indicative of this. Thus, EMPA regulated the XBP1s/XBP1u protein ratio through downregulation of cleaved ATF6α and upregulation of IRE1.

Results of the present study demonstrated an induction of ER stress in Dox-treated cardiomyocytes. As prolonged ER stress mediates cardiomyocyte apoptosis (13,24,42), the expression of ER-initiated apoptotic markers were examined. An overexpression of ER-resident caspase-12 and cleaved caspase-12 was observed following Dox treatment, and these expression levels were significantly reduced following pre-treatment with EMPA. Cleaved caspase-12 acts as a precursor of the activation of caspase-3-induced apoptosis (14). EMPA exerts an inhibitory effect on caspase-induced apoptosis and subsequent cell death in both renal and myocardial I/R injury (38,43). Expression of the downstream signaling molecule, JNK, and the subsequent phosphorylation is involved in ER stress-induced apoptosis and autophagy in fibroblast or in cancer cells via the IRE1-JNK pathway (42,44). Although the activation of IRE1 was not observed following Dox treatment, phosphorylation of JNK

was increased, suggesting ER-independent activation. EMPA inhibits IL-1β (45), which may play an important role in the inhibition of inflammation, JNK-induced apoptosis and thus, the promotion of cellular homeostasis. The effect of EMPA on apoptosis was evident through the significant increase in the viability of Dox-treated cardiomyocytes.

DIC is also mediated via increased OS and inflammation that leads to cardiomyocyte apoptosis. Results of the EMPA's effects in patients with type 2 diabetes mellitus and coronary artery disease (EMPA-CARD) trial demonstrated that 6 months of treatment with EMPA significantly mitigated inflammation, OS and platelet activity in patients with diabetes and coronary artery disease (46). In the present study, 1 h of pre-treatment with EMPA significantly reduced OS, compared with the Dox treatment group. Results of the present study also demonstrated a significant increase in the levels of *TNFα* under Dox treatment; however, pre-treatment with EMPA reduced *TNFα* levels in the Dox + EMPA group. Notably, EMPA improved renal ischemia/reperfusion injury in non-diabetic rats through the TNFα signaling pathway (43). Dox treatment significantly reduced *IL-10* levels, which exert anti-inflammatory and anti-oxidant effects in the heart (47,48). Results of the present study also revealed an increase in *TGFβ* mRNA levels in the Dox group, and expression was reduced following treatment with EMPA. Inhibition of *TGFβ* signalling in cardiac endothelial cells exerts cardioprotective effects and mitigates DIC (49,50). Results of a previous study demonstrated that inhibition of SGLT2 was beneficial in mitigating fibrosis in a model of myocardial ischemia (51). Thus, EMPA-induced inhibition of *TGFβ* expression may protect the heart from Dox-induced fibrosis. In addition, STAT-3 plays a beneficial role in the heart through upregulating anti-oxidants, anti-apoptotic genes and mediating inflammation (52). Notably, *STAT-3* expression was downregulated following Dox treatment (53). However, EMPA significantly increased *STAT-3* expression levels, thus maintaining the redox state and inflammation in Dox-treated cardiomyocytes. Another SGLT2 inhibitor, Dapagliflozin, also reduces DIC via restoring STAT-3 levels (54). The beneficial effects of EMPA on the restoration of STAT-3 protein expression may promote cardiomyocyte proliferation, maintain the redox state, and protect the heart from cardiac inflammation.

In conclusion, ER is associated with cardiac function in a number of cardiovascular diseases (55,56). *In vitro*, EMPA mitigated ER stress in DIC via the IRE1-ATF6α pathway, and subsequent reduced OS, inflammation and cardiomyocyte apoptosis. Further investigations are required to evaluate the cardioprotective role of EMPA and the associated mechanisms in both the prevention and treatment of DIC.

Notably, the present study exhibits numerous limitations. For example, SGLT2s are not the only glucose transporters present in the heart, as the heart primarily relies on GLUT1 and GLUT4 for glucose uptake. Therefore, the inhibition of GLUT1 and GLUT4 may provide further insights into the direct role of SGLT2 in DIC. The present study was focused on Dox-induced ER stress and ER stress-induced apoptosis and investigated the potential beneficial effects of EMPA in inhibiting ER stress. However, DIC is multifaceted, and further investigations into the cardioprotective role of EMPA in Dox-induced injury are required. Additionally, *in vivo* studies are required to determine the efficacy of EMPA in protecting heart damage, without interfering with the anticancer properties of Dox.

Acknowledgements

Not applicable.

Funding

The present study was supported by operating grants from the Heart and Stroke Foundation of Canada (grant no. G-19-0024241), the Molson Women's Heart Health Program (grant no. 2003-31-94-c), and the CANUSA grant (grant no. R510867).

Availability of data and materials

The datasets used and/or analyzed during the current study are available from the corresponding author on reasonable request.

Authors' contributions

AM and PKS conceived and designed the research study. AM completed all of the experiments and acquired data. AM and DSJ confirm the authenticity of all the raw data. PKS and DSJ provided resources and materials. AM, AKB, PKS and DSJ contributed to data analysis and writing and editing the manuscript. All authors have read and approved the final version of the manuscript.

Ethics approval and consent to participate

The animal experimental procedures were performed per the guidelines of the Canadian Council on Animal Care for all animal procedures, including animal handling and drug administration as approved [approval no. (22-012 (AC11739)] by the Animal Protocol Review Committee at the University of Manitoba (Winnipeg, Canada).

Patient consent for publication

Not applicable.

Competing interests

The authors declare that they have no competing interests.

References

1. Lefrak EA, Pitha J, Rosenheim S and Gottlieb JA: A clinicopathologic analysis of adriamycin cardiotoxicity. Cancer 32: 302-314, 1973.
2. Singal PK and Iliskovic N: Doxorubicin-induced cardiomyopathy. N Engl J Med 339: 900-905, 1998.
3. Ludke AR, Sharma AK, Akolkar G, Bajpai G and Singal PK: Downregulation of vitamin C transporter SVCT-2 in doxorubicin-induced cardiomyocyte injury. Am J Physiol Cell Physiol 303: C645-C653, 2012.
4. Singal PK, Siveski-Iliskovic N, Hill M, Thomas TP and Li T: Combination therapy with probucol prevents adriamycin-induced cardiomyopathy. J Mol Cell Cardiol 27: 1055-1063, 1995.

5. Torti FM, Bristow MM, Lum BL, Carter SK, Howes AE, Aston DA, Brown BW Jr, Hannigan JF Jr, Meyers FJ, Mitchell EP, *et al*: Cardiotoxicity of epirubicin and doxorubicin: Assessment by endomyocardial biopsy. Cancer Res 46: 3722-3727, 1986.
6. Singal PK, Deally CM and Weinberg LE: Subcellular effects of adriamycin in the heart: A concise review. J Mol Cell Cardiol 19: 817-828, 1987.
7. Krebs J, Agellon LB and Michalak M: Ca(2+) homeostasis and endoplasmic reticulum (ER) stress: An integrated view of calcium signaling. Biochem Biophys Res Commun 460: 114-121, 2015.
8. Hetz C and Papa FR: The unfolded protein response and cell fate control. Mol Cell 69: 169-181, 2018.
9. Harding HP, Zhang Y, Bertolotti A, Zeng H and Ron D: Perk is essential for translational regulation and cell survival during the unfolded protein response. Mol Cell 5: 897-904, 2000.
10. Glembotski CC: Roles for ATF6 and the sarco/endoplasmic reticulum protein quality control system in the heart. J Mol Cell Cardiol 71: 11-15, 2014.
11. Yoshida H, Matsui T, Yamamoto A, Okada T and Mori K: XBP1 mRNA is induced by ATF6 and spliced by IRE1 in response to ER stress to produce a highly active transcription factor. Cell 107: 881-891, 2001.
12. Bertolotti A, Zhang Y, Hendershot LM, Harding HP and Ron D: Dynamic interaction of BiP and ER stress transducers in the unfolded-protein response. Nat Cell Biol 2: 326-332, 2000.
13. Bagchi AK, Malik A, Akolkar G, Zimmer A, Belló-Klein A, De Angelis K, Jassal DS, Fini MA, Stenmark KR and Singal PK: Study of ER stress and apoptotic proteins in the heart and tumor exposed to doxorubicin. Biochim Biophys Acta Mol Cell Res 1868: 119039, 2021.
14. Hitomi J, Katayama T, Taniguchi M, Honda A, Imaizumi K and Tohyama M: Apoptosis induced by endoplasmic reticulum stress depends on activation of caspase-3 via caspase-12. Neurosci Lett 357: 127-130, 2004.
15. Hsia DS, Grove O and Cefalu WT: An update on sodium-glucose co-transporter-2 inhibitors for the treatment of diabetes mellitus. Curr Opin Endocrinol Diabetes Obes 24: 73-79, 2017.
16. Zinman B, Wanner C and Lachin JM; EMPA-REG OUTCOME Investigators: Empagliflozin, cardiovascular outcomes, and mortality in type 2 diabetes. N Engl J Med 373: 2117-2128, 2015.
17. Butler J, Anker SD, Filippatos G, Khan MS, Ferreira JP, Pocock SJ, Giannetti N, Januzzi JL, Piña IL, Lam CSP, *et al*: Empagliflozin and health-related quality of life outcomes in patients with heart failure with reduced ejection fraction: The EMPEROR-reduced trial. Eur Heart J 42: 1203-1212, 2021.
18. Packer M, Anker SD, Butler J, Filippatos G, Pocock SJ, Carson P, Januzzi J, Verma S, Tsutsui H, Brueckmann M, *et al*: Cardiovascular and Renal outcomes with empagliflozin in heart failure. N Engl J Med 383: 1413-1424, 2020.
19. Anker SD, Butler J, Filippatos G, Ferreira JP, Bocchi E, Böhm M, Brunner-La Rocca HP, Choi DJ, Chopra V, Chuquiure-Valenzuela E, *et al*: Empagliflozin in heart failure with a preserved ejection fraction. N Engl J Med 385: 1451-1461, 2021.
20. McDonald M, Virani S, Chan M, Ducharme A, Ezekowitz JA, Giannetti N, Heckman GA, Howlett JG, Koshman SL, Lepage S, *et al*: CCS/CHFS heart failure guidelines update: Defining a new pharmacologic standard of care for heart failure with reduced ejection fraction. Can J Cardiol 37: 531-546, 2021.
21. Sabatino J, De Rosa S, Tammè L, Iaconetti C, Sorrentino S, Polimeni A, Mignogna C, Amorosi A, Spaccarotella C, Yasuda M and Indolfi C: Empagliflozin prevents doxorubicin-induced myocardial dysfunction. Cardiovasc Diabetol 19: 66, 2020.
22. Chang WT, Lin YW, Ho CH, Chen ZC, Liu PY and Shih JY: Dapagliflozin suppresses ER stress and protects doxorubicin-induced cardiotoxicity in breast cancer patients. Arch Toxicol 95: 659-671, 2021.
23. Bagchi AK, Malik A, Akolkar G, Jassal DS and Singal PK: Endoplasmic reticulum stress promotes iNOS/NO and influences inflammation in the development of doxorubicin-induced cardiomyopathy. Antioxidants (Basel) 10: 1897, 2021.
24. Malik A, Bagchi AK, Jassal DS and Singal PK: Interleukin-10 mitigates doxorubicin-induced endoplasmic reticulum stress as well as cardiomyopathy. Biomedicines 10: 890, 2022.
25. Zhao L and Zhang B: Doxorubicin induces cardiotoxicity through upregulation of death receptors mediated apoptosis in cardiomyocytes. Sci Rep 7: 44735, 2017.
26. Yarmohammadi F, Rezaee R, Haye AW and Karimi G: Endoplasmic reticulum stress in doxorubicin-induced cardiotoxicity may be therapeutically targeted by natural and chemical compounds: A review. Pharmacol Res 164: 105383, 2021.
27. Livak KJ and Schmittgen TD: Analysis of relative gene expression data using real-time quantitative PCR and the 2(-Delta Delta C(T)) Method. Methods 25: 402-408, 2001.
28. Heidenreich PA, Bozkurt B, Aguilar D, Allen LA, Byun JJ, Colvin MM, Deswal A, Drazner MH, Dunlay SM, Evers LR, *et al*: 2022 AHA/ACC/HFSA Guideline for the Management of Heart Failure: A Report of the American College of Cardiology/American Heart Association Joint Committee on Clinical Practice Guidelines. Circulation 145: e89-e1032, 2022.
29. Di Franco A, Cantini G, Tani A, Coppini R, Zecchi-Orlandini S, Raimondi L, Luconi M and Mannucci E: Sodium-dependent glucose transporters (SGLT) in human ischemic heart: A new potential pharmacological target. Int J Cardiol 243: 86-90, 2017.
30. Chen J, Williams S, Ho S, Loraine H, Hagan D, Whaley JM and Feder JN: Quantitative PCR tissue expression profiling of the human SGLT2 gene and related family members. Diabetes Ther 1: 57-92, 2010.
31. Zhou L, Cryan EV, D'Andrea MR, Belkowski S, Conway BR and Demarest KT: Human cardiomyocytes express high level of Na+/glucose cotransporter 1 (SGLT1). J Cell Biochem 90: 339-346, 2003.
32. Kashiwagi Y, Nagoshi T, Yoshino T, Tanaka TD, Ito K, Harada T, Takahashi H, Ikegami M, Anzawa R and Yoshimura M: Expression of SGLT1 in human hearts and impairment of cardiac glucose uptake by phlorizin during ischemia-reperfusion injury in mice. PLoS One 10: e0130605, 2015.
33. Quagliariello V, De Laurentiis M, Rea D, Barbieri A, Monti MG, Carbone A, Paccone A, Altucci L, Conte M, Canale ML, *et al*: The SGLT-2 inhibitor empagliflozin improves myocardial strain, reduces cardiac fibrosis and pro-inflammatory cytokines in non-diabetic mice treated with doxorubicin. Cardiovasc Diabetol 20: 150, 2021.
34. Nakano D, Akiba J, Tsutsumi T, Kawaguchi M, Yoshida T, Koga H and Kawaguchi T: Hepatic expression of sodium-glucose cotransporter 2 (SGLT2) in patients with chronic liver disease. Med Mol Morphol 55: 304-315, 2022.
35. Bertero E and Maack C: Metabolic remodelling in heart failure. Nat Rev Cardiol 15: 457-470, 2018.
36. Asnani A, Shi X, Farrell L, Lall R, Sebag IA, Plana JC, Gerszten RE and Scherrer-Crosbie M: Changes in citric acid cycle and nucleoside metabolism are associated with anthracycline cardiotoxicity in patients with breast cancer. J Cardiovasc Transl Res 13: 349-356, 2020.
37. Fu HY, Sanada S, Matsuzaki T, Liao Y, Okuda K, Yamato M, Tsuchida S, Araki R, Asano Y, Asanuma H, *et al*: Chemical endoplasmic reticulum chaperone alleviates doxorubicin-induced cardiac dysfunction. Circ Res 118: 798-809, 2016.
38. Wang CC, Li Y, Qian XQ, Zhao H, Wang D, Zuo GX and Wang K: Empagliflozin alleviates myocardial I/R injury and cardiomyocyte apoptosis via inhibiting ER stress-induced autophagy and the PERK/ATF4/Beclin1 pathway. J Drug Target 30: 858-872, 2022.
39. Hetz C: The unfolded protein response: Controlling cell fate decisions under ER stress and beyond. Nat Rev Mol Cell Biol 13: 89-102, 2012.
40. Lee AH, Iwakoshi NN and Glimcher LH: XBP-1 regulates a subset of endoplasmic reticulum resident chaperone genes in the unfolded protein response. Mol Cell Biol 23: 7448-7459, 2003.
41. Yoshida H, Oku M, Suzuki M and Mori K: pXBP1(U) encoded in XBP1 pre-mRNA negatively regulates unfolded protein response activator pXBP1(S) in mammalian ER stress response. J Cell Biol 172: 565-575, 2006.
42. Kato H, Nakajima S, Saito Y, Takahashi S, Katoh R and Kitamura M: mTORC1 serves ER stress-triggered apoptosis via selective activation of the IRE1-JNK pathway. Cell Death Differ 19: 310-320, 2012.
43. Ala M, Khoshdel MRF and Dehpour AR: Empagliflozin enhances autophagy, mitochondrial biogenesis, and antioxidant defense and ameliorates renal ischemia/reperfusion in nondiabetic rats. Oxid Med Cell Longev 2022: 1197061, 2022.
44. Haberzettl P and Hill BG: Oxidized lipids activate autophagy in a JNK-dependent manner by stimulating the endoplasmic reticulum stress response. Redox Biol 1: 56-64, 2013.
45. Pirklbauer M, Sallaberger S, Staudinger P, Corazza U, Leierer J, Mayer G and Schramek H: Empagliflozin inhibits IL-1beta-mediated inflammatory response in human proximal tubular cells. Int J Mol Sci 22: 5089, 2021.

46. Gohari S, Reshadmanesh T, Khodabandehloo H, Karbalaee-Hasani A, Ahangar H, Arsang-Jang S, Ismail-Beigi F, Dadashi M, Ghanbari S, Taheri H, *et al*: The effect of EMPAgliflozin on markers of inflammation in patients with concomitant type 2 diabetes mellitus and coronary ARtery disease: The EMPA-CARD randomized controlled trial. Diabetol Metab Syndr 14: 170, 2022.
47. Bagchi AK, Surendran A, Malik A, Jassal DS, Ravandi A and Singal PK: IL-10 attenuates OxPCs-mediated lipid metabolic responses in ischemia reperfusion injury. Sci Rep 10: 12120, 2020.
48. Dhingra S, Sharma AK, Arora RC, Slezak J and Singal PK: IL-10 attenuates TNF-alpha-induced NF kappaB pathway activation and cardiomyocyte apoptosis. Cardiovasc Res 82: 59-66, 2009.
49. Sun Z, Schriewer J, Tang M, Marlin J, Taylor F, Shohet RV and Konorev EA: The TGF-β pathway mediates doxorubicin effects on cardiac endothelial cells. J Mol Cell Cardiol 90: 129-138, 2016.
50. Li J, Deane JA, Campanale NV, Bertram JF and Ricardo SD: Blockade of p38 mitogen-activated protein kinase and TGF-beta1/Smad signaling pathways rescues bone marrow-derived peritubular capillary endothelial cells in adriamycin-induced nephrosis. J Am Soc Nephrol 17: 2799-2811, 2006.
51. Li G, Zhao C and Fang S: SGLT2 promotes cardiac fibrosis following myocardial infarction and is regulated by miR-141. Exp Ther Med 22: 715, 2021.
52. Lim CP and Fu XY: Multiple roles of STAT3 in cardiovascular inflammatory responses. In: Progress in Molecular Biology and Translational Science. Vol 106. Shenolikar S (ed). Academic Press, pp63-73, 2012.
53. de Oliveira Santos TC, Pereira G, Coutinho AGG, Dos Santos Silva HP, Lima MMS, Dias FAL, de Almeida DC, Resende E Silva DT, Perez RF and Pereira RL: STAT-3 signaling role in an experimental model of nephropathy induced by doxorubicin. Mol Cell Biochem 478: 981-989, 2023.
54. Chang WT, Shih JY, Lin YW, Chen ZC, Kan WC, Lin TH and Hong CS: Dapagliflozin protects against doxorubicin-induced cardiotoxicity by restoring STAT3. Arch Toxicol 96: 2021-2032, 2022.
55. Dufey E, Sepúlveda D, Rojas-Rivera D and Hetz C: Cellular mechanisms of endoplasmic reticulum stress signaling in health and disease. 1. An overview. Am J Physiol Cell Physiol 307: C582-C594, 2014.
56. Gaut JR and Hendershot LM: The modification and assembly of proteins in the endoplasmic reticulum. Curr Opin Cell Biol 5: 589-595, 1993.